0.1 Physical observables: timing residuals

The principle observational quantify reported on for a pulsar is the timing residual. This is measured by the difference between the TOA of a pulse and a timing model of the pulsar. It is the quasi-periodic structure in the timing residual which we term timing-noise and hence we naturally want to be able to calculate the residual from our analytic models.

Using equation (**??**) we can calculate the exact phase evolution of the star given the relevant Euler angles and components of the spin-vector; we will label this as $\Phi_{\rm exact}$. Following the methods used by observers, we take a Taylor expansion to the phase about some fixed time t_0

$$\Phi(t; t_0, \phi, f, \dot{f}, \ddot{f}) = \phi + 2\pi \left(f(t-t_0) + \frac{\dot{f}}{2!}(t-t_0)^2 + \frac{\ddot{f}}{3!}(t-t_0)^3 \right), \tag{0.1.1}$$

and use a least-squares fitting method to minimise the squared error between the Taylor expansion and $\Phi_{\rm exact}$. The resulting coefficients $\{\phi_0, f_0, \dot{f}_0, \ddot{f}_0\}$ are the quantities best describing the NS under a power law spindown. In pulsar astronomy these are referred to as the timing model. We will refer to the best-fit phase as described by these coefficients as

$$\Phi_{\rm fit}(t) = \Phi(t; t_0, \phi_0, f_0, \dot{f}_0, \ddot{f}_0) \tag{0.1.2}$$

The phase-residual is then defined as the difference between the exact phase and the fitted phase

$$\Delta\Phi(t) = \Phi_{\rm exact}(t) - \Phi_{\rm fit}(t). \tag{0.1.3}$$

It is worth noting that a phase residual depends on the fit to the entire length of date provided in $\Phi_{\rm exact}$.

The phase residual can be re-scaled to give the timing residual by calculating the residual as a fraction of a cycle then multiplying by the period

$$\Delta T = \frac{\Delta\Phi(t)}{2\pi} P. \tag{0.1.4}$$

Over a typical observation periods it is possible for the period to fractionally change due to the spindown. For this work we will report only on phase-residuals although to make contact with observational results we will require this re-scaling.

0.1.1 Verifying the simulated timing residuals

The effect of free-precession and the inclusion of an EM torque was considered analytically by **?**. They calculated several useful results for the magnitude of variations in the residual; we can use these to verify our simulations. By simulating the residuals directly, we can improve on their results by understanding some of the more subtle features.

0.1.2 Understanding the wobble angle

The analytic calculations of **?** are based on the wobble angle $\tilde{\theta}$ which the spin-vector makes with the axis about which it precesses. This axis depends on the mass distribution, and any applied torques. Before continuing we discuss what this wobble angle is given by in different cases.

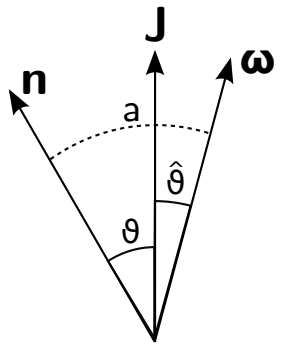

Figure 0.1.1: The reference plane containing the angular momentum vector $\boldsymbol{\omega}$, the angular momentum vector Ł and the symmetry axis n lying along the body-frame $\hat{\boldsymbol{z}}$ axis. The dotted line indicates the polar angle a between the body-frame $\hat{\boldsymbol{z}}$ axis and the spin vector.

To understand the wobble angle we refer to figure 0.1.1 illustrating the so-called reference plane from **?** This reference plane is a direct result of the relation

$$L_a = I_{ab}\omega_b \qquad\qquad I_{ab} = I_0\delta_{ab} + \epsilon_{\rm I}\delta_{3a}\delta_{3b} \tag{0.1.5}$$

since **n** lies along the $\hat{\boldsymbol{z}}$ axis of the body frame. It was shown by **?** that for nearly spherical bodies

$$\hat{\theta} \approx \epsilon_{\rm I} \sin\theta\cos\theta. \tag{0.1.6}$$

Taking also the limit that $\theta \ll 1$ it can be shown that

$$\hat{\theta} \approx \epsilon_{\rm I}\theta \tag{0.1.7}$$

and so when comparing the two angles $\hat{\theta} \ll \theta$ such that $a \approx \theta$.

For a biaxial body free of torques, the spin vector precesses about the symmetry axis of the moment of inertia **n**. Using the approximations mentioned above then the wobble angle is given by

$$\tilde{\theta} \approx \theta. \tag{0.1.8}$$

Therefore, solutions without precession correspond to $a = 0$.

Including the EM torque from equation (**??**) introduces two effects: the first and the largest is the transformation induced by the anomalous torque which causes the spin-vector to precess about the principle axis of an *effective* body-frame. This has already been discussed in chapter **??** and results in a wobble angle

$$\tilde{\theta} \approx \theta - \beta \tag{0.1.9}$$

where β is the rotation from the body-frame to the effective body-frame. In this case non-precessing solutions correspond to $a \approx \beta$.

The second, smaller effect is that, even without the anomalous torque the spin-down torque introduces a time-varying component to the angular momentum vector. Which will change the axis of precession. The magnitude of this time varying component is given by

$$|\dot{\text{Ł}}| \sim L\omega\hat{\theta} \tag{0.1.10}$$

this can be equated to the magnitude of the spindown torque

$$|T_{\rm sd}| = I_0|\dot{\boldsymbol{\omega}}| \tag{0.1.11}$$

rearranging for the angle between the spin-vector and angular momentum yeilds

$$\hat{\theta} = \frac{I_0 \dot{\omega}}{I\omega^2} = \frac{P}{\tau_{\rm S}} \tag{0.1.12}$$

The wobble angle due to this spin-down torque is then given by

$$\begin{aligned}
\tilde{\theta}_{\rm SD} &= \theta + \hat{\theta} && (0.1.13)\\
&= \hat{\theta}\left(1 + \frac{1}{\epsilon_{\rm I}}\right) && (0.1.14)\\
&= \frac{P}{\tau_{\rm S}}\left(1 + \frac{1}{\epsilon_{\rm I}}\right) && (0.1.15)\\
&\approx \frac{P}{\tau_{\rm S}}\frac{1}{\epsilon_{\rm I}} && (0.1.16)
\end{aligned}$$

Therefore we can write the wobble angle in general as

$$\tilde{\theta} = \theta - \beta + \frac{P}{\tau_{\rm S}}\frac{1}{\epsilon_{\rm I}} \tag{0.1.17}$$

Now for solutions where the precession is important the final term will be negligable and so we generally refer to equation (0.1.9). However, when we set up initial conditions to minimise the precession: either $a_0 = 0$ for free precession or $a_0 = \beta$ when incuding the anomalous torque; the approximations we made earlier become important. Now the wobble angle due to the spindown can dominate and so we should use the full expression in equation (0.1.17).

Effect of free precession on the phase residual: geometric effect

? analysed the geometric effect that precession will have on the timing residual. This was done by considering the motion of the magnetic dipole in the inertial frame as the superposition of motions due to the fast rotation period and the slow precession. The results must be separated into two cases when $\theta > \chi$ and $\theta < \chi$. Of these two the authors argue that 'the wobble angle of rapidly rotating stars are limited to small values by the finite crustal breaking strain'. Therefore, the second case $\theta < \chi$ holds greater physical relevance and so we focus on this region of parameter space. The phase residual for such NSs was shown to be given by

$$\Delta\Phi^{49}(t) = -\tilde{\theta}\cot\chi\cos(\dot{\psi}t), \tag{0.1.18}$$

where the superscript here refers to the equation number from **?**. For a freely precession star $\dot{\psi} = \epsilon_{\rm I} f$ is the constant free precession frequency. Therefore, the magnitude of variations is given by $|\Delta\Phi^{49}| = \tilde{\theta}\cot(\chi)$.

Equation (0.1.18) is calculated in the absence of any EM torque. Nevertheless, it is still appropriate when such a torque is applied provided that the geometric effect is stronger that any other (these are discussed in the next few sections). As such we begin by simulating a NS with the properties listed in table 0.1.1. Nonphysical values of the rotation frequency and magnetic field have been used to aid the computational speed. The resulting phase residual, in cycles, is given in figure 0.1.2.

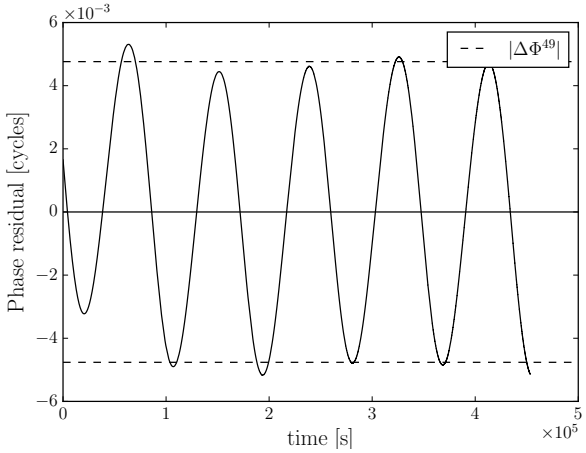

Figure 0.1.2: The phase residual in cycles for a simulated NS with the properties described in table 0.1.1. This is used to illustrate the agreement with the magnitude of variations from equation (0.1.18) taken from **?**.

Simulation parameters		
ω_0	=	15.5 rad/s
B_0	=	1.581×10^{14} G
χ	=	49.99°
a_0	=	2.00°
$\tilde{\theta}$	=	2.04°
$\mathcal{A}_{\rm EM}$	=	0.41

Table 0.1.1

Effect of free precession on the phase residual: effect of the electromagnetic torque

Considering a vacuum point-dipole spin-down torque (like the one introduced in **??**) **?** found that the EM torque can amplify the geometric effect of equation (0.1.18). The magnitude of variation due to EM torque is given by

$$|\Delta\Phi^{63}| = \frac{1}{\pi}\left(\frac{\tau_P}{P}\right)\left(\frac{\tau_P}{\tau_S}\right)|\Delta\Phi^{49}| \tag{0.1.19}$$

The two ratios of time-scales define an 'amplification factor':

$$\mathcal{A}_{\rm EM} = \left(\frac{\tau_P}{P}\right)\left(\frac{\tau_P}{\tau_S}\right) \tag{0.1.20}$$

The amplification increases the magnitude of phase residuals for young pulsars with short periods.

We simulate such a star using the properties in table 0.1.2 noting that the amplification factor is ~ 3 when including the factor of π. The resulting phase residual is plotted in figure 0.1.3 along with the magnitude of variations due to free precession along and the amplification due to the EM torque. The magnitude of the simulated phase-residuals are found to agree well with the analytic results of equation (0.1.19).

Effect of free precession on phase residuals: orthogonal rotator

In analysing observations of free precession **?** applied the model to PSR B1821-11: a pulsar with a strongly periodic residual that has been cited as a strong candidate for free precession **?**. From the variations in pulse shape an estimate can be made of the wobble angle $\tilde{\theta} \sim 3°$. Finding that the amplification factor was important for this pulsar (it can be calculated to be ≈ 380), **?** attempted to extract the wobble angle by inverting (0.1.19). This yields a wobble angle that disagreed with the estimation from a pulse shape variations. The author concluded that the strong harmonic

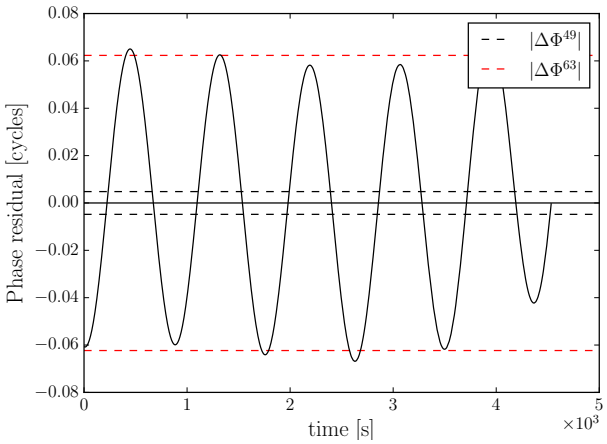

Figure 0.1.3: The phase residual in cycles for a simulated NS with the properties described in table 0.1.2. This is used to illustrate the agreement with the magnitude of variations from equation (0.1.19) taken from **?**.

Simulation parameters		
ω_0	=	1550.0 rad/s
B_0	=	1.581×10^{14} G
χ	=	49.99°
a_0	=	2.00°
$\tilde{\theta}$	=	2.06°
$\mathcal{A}_{\rm EM}$	=	41.0

Table 0.1.2

periodicity's suggested the dipole was nearly orthogonal e.g. $\chi \approx \pi/2$. This required expansions of the phase modulation resulting in an estimate

$$|\Delta\Phi^{75}| = \frac{1}{4\pi}\frac{\tau_P^2}{\tau_S P}\theta^2 \tag{0.1.21}$$

In figure 0.1.4 we simulate the B1828-11 pulsar taking the values from **?** and modifying them to allow the simulation to complete in a reasonable time. The modification was setup such that the amplification factor remained the same along with the ratio of timescales. The properties of the simulation are given in 0.1.3

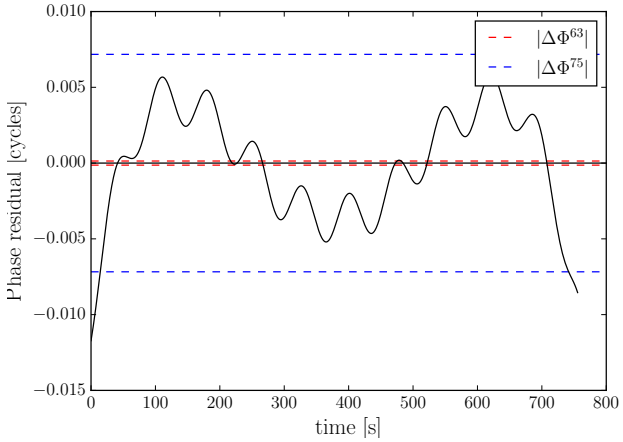

Figure 0.1.4: The phase residual in cycles for a simulated NS with the properties described in table 0.1.3. This is used to illustrate the agreement with the magnitude of variations from equation (0.1.21) taken from **?**.

Simulation parameters		
ω_0	=	9310.0 rad/s
B_0	=	1.581×10^{14} G
χ	=	89.99°
a_0	=	2.00°
$\tilde{\theta}$	=	2.11°
$\mathcal{A}_{\rm EM}$	=	420.0

Table 0.1.3

0.1.3 Single torque switching events

The recent observations by **?** suggest that for a few pulsars the quasi-periodic structure observed in pulsar timing residuals is a result of torque-switching events. They find that the spin-down periodically switches between two distinct values and these changes correlate with changes in the beam width. They argue this indicates that the electromagnetic torque is periodically switching between two distinct states.

We will not discuss where the periodic nature comes from here, but instead present a direct simulation of the timing residuals from switching events. For simplicity we begin by consider a single switch in the torque at some time $t_{\rm switch}$; for the time being we set this to be half the observation period, such that $t_{\rm switch} = T_{\rm obs}/2$.

In the EM dipole spindown model the torque has two distinct components: the regular spin-down part and the so-called anomalous component. This later term does not contribute to the spin-down, but as discussed in section **??** it will modify the axis of precession. The torque switching will occur in the spin-down component, but it seems unlikely that it will also occur in the anomalous component [Ian - why?]. To cover all cases we model a single torque switching effect by redefining the torque in equation (**??**) such that

$$\mathbf{T} = (1 - S_{\rm S} H(t - t_{\rm switch}))\mathbf{T}_{\rm S} + (1 - S_{\rm A} H(t - t_{\rm switch}))\mathbf{T}_{\rm A} \tag{0.1.22}$$

where the subscripts label the spin-down and anomalous components, S is the strength of switching, and $H(t)$ is the Heaviside function.

Numerically solving the body-frame and Euler equations using this torque we simulate a single switching event to try and understand the effect it will have on phase residuals.

Minimal precession

Without the torque-switching, in these simulations only free precession can produce structure in the phase residuals. No pulsars exist with regular periodic structure that can be solely interpreted

as free precession. Most pulsars must therefore exist with very small wobble angles with any excitement of this being damped. As such, we begin by discussing the "minimal precession" initial conditions from which to start our simulations.

Precession will not occur when the spin vector is aligned with the axis about which it rotates. The angle between these two we have defined as the wobble angle. For minimal precession we should therefore set this wobble angle to zero. In all simulations we consider a biaxial body with the full torque given in (0.1.22). From our previous discussion on the wobble angle we can minimise the precession by setting the initial polar angle of the spin vector in the body frame to lie along the effective body-frame axis. That is

$$a_0 = \beta(\epsilon_{\rm I}, \epsilon_{\rm A}, \chi), \tag{0.1.23}$$

we refer to such a simulation as 'minimal precession' since the wobble angle remains non-zero.

In this case the wobble angle will given by equation (0.1.16): The magnitude of variations in the phase-residuals is given by inserting this wobble angle

$$\tilde{\theta} \approx \frac{1}{\epsilon_{\rm I}} \frac{P}{\tau_{\rm S}} \tag{0.1.24}$$

into either equation (0.1.18) or (0.1.21) depending on the EM amplification factor.

We verify this by setting up a minimal precession simulation. The resulting phase residual is given in figure 0.1.5 along with the predicted magnitude of variations. In table 0.1.4 we give the simulation properties: note that the initial polar angle is exactly the angle β which can be calculated using equation (**??**). The wobble angle is given by equation (0.1.17) and is non-zero due to the spindown torque.

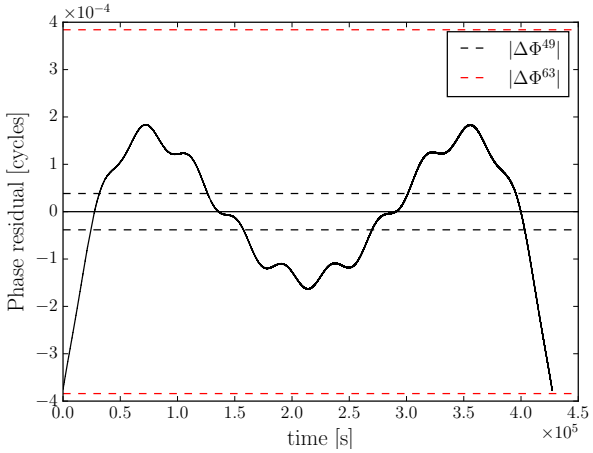

Figure 0.1.5

Simulation parameters		
ω_0	=	15.0 rad/s
B_0	=	2.683×10^{15} G
χ	=	60.10°
a_0	=	-4.46°
$\tilde{\theta}$	=	0.02°
$\mathcal{A}_{\rm EM}$	=	31.0

Table 0.1.4

We will now setup a simulation of this 'minimal precession' NS, and then manually switch the torque. We choose a NS where the EM torque amplification given in equation (0.1.21) is important.

0.1.4 Switching without the anomalous torque

We now consider manually switching the spindown torque halfway though the simulation. That is we set

$$t_{\rm switch} = \frac{T_{\rm obs}}{2}, \qquad S_{\rm S} = 0.4, \qquad S_{\rm A} = 0.0, \tag{0.1.25}$$

such that halfway though the simulation the spindown torque is reduced by a fraction 0.4 while the anomalous torque remains unaffected.

In figure 0.1.6 we plot the phase residuals from this simulation. In the top plot is the residual as calculated over the entire observation period. We find a single periodic variation with significantly larger variation than any of the precession features. This is a direct result of the switching only as discussed in section **??**: the effect of precession is entirely swamped by the switching. For this reason in the lower plot we calculate two residuals: the first is calculated in the region $[0, t_{\rm switch}]$ and the second in $[t_{\rm switch}, T_{\rm obs}]$. Because the switch does not occur in either of these periods we can resolve the free precession during each period.

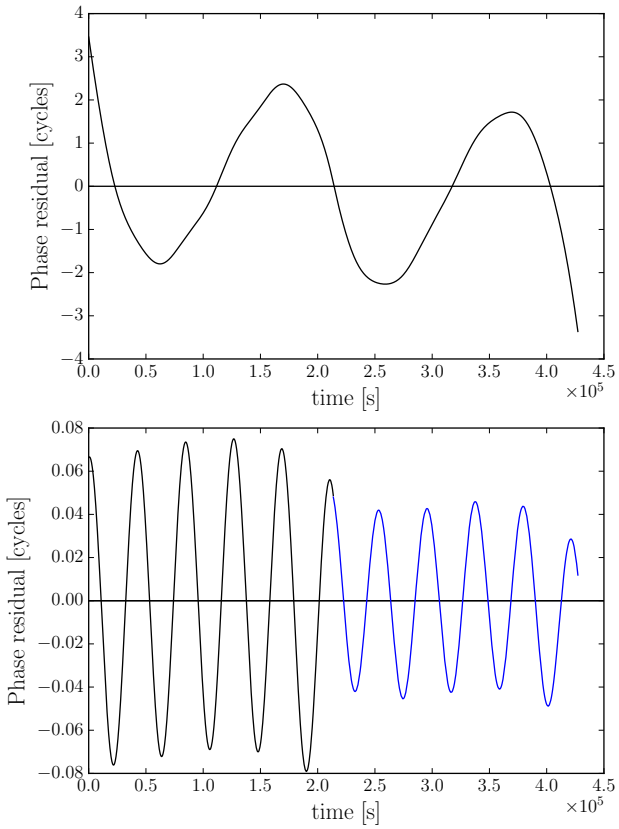

Figure 0.1.6

The simulations begin in the minimal precession state where the spin-vector is aligned with the effective body frame axis such that the wobble angle is given by equation (0.1.16). After the switch, the wobble angle is smaller by a factor $S_{\rm S}$ and as a result we see the precession is reduced by this fraction.

0.1.5 Switching with the anomalous torque

We now consider manually switching both the spindown and anomalous torque halfway though the simulation. That is we set

$$t_{\text{switch}} = \frac{T_{\text{obs}}}{2}, \qquad S_{\text{S}} = S_{\text{A}} = 0.01 \tag{0.1.26}$$

In a similar fashion to figure 0.1.6 we show first the total residual in the top plot of figure 0.1.7, and then the individual residuals in the lower plot.

In this simulation we have used a significantly smaller switching fraction than when switching without the anomalous torque. This is because the effect on the phase residuals when calculated in the two regions is significantly stronger. This is because we begin with a 'minimal precession' state, where $\theta = \beta$ and the precession results from effect of the spin-down torque. Then, when we switching off a fraction of the anomalous torque we have modified the effective body frame and hence the angle β. This generates a significantly larger wobble angle producing a significant increase in the phase residuals fitted in the post-switch period. The effect is not observable when fitting to the entire simulation period since the switching event remains dominant.

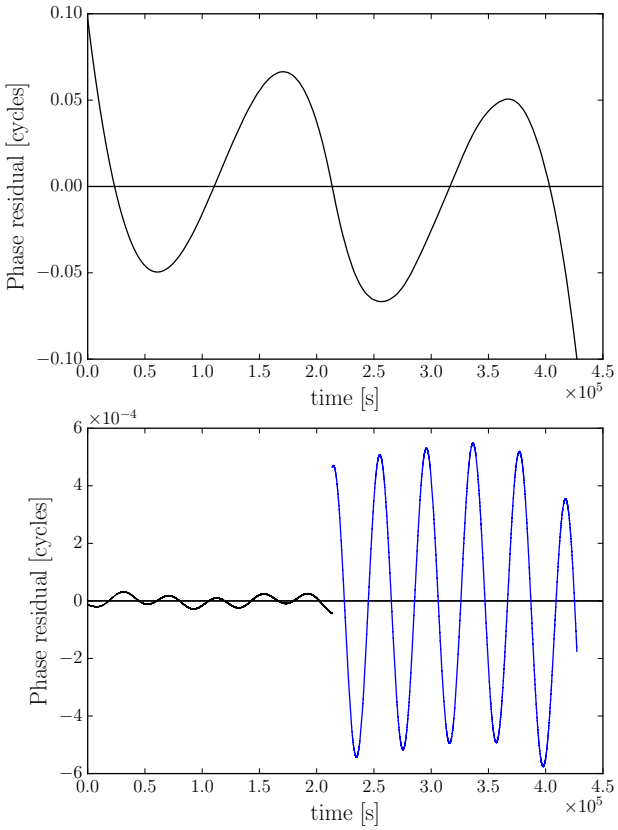

Figure 0.1.7

Calculating the new wobble angle after a switch

We now calculate the change in wobble angle and hence phase-residual variations after switching a fraction of the anomalous torque. In our model the strength of the torque is parameterised by $\epsilon_{\rm A}$, related to the surface magnetic field strength by

$$\epsilon_{\rm A} = \frac{R^5}{4I_0c^2}B_0^2. \tag{0.1.27}$$

Rearranging equation (1.4.8) of my transfer thesis we can then write the spindown as

$$\dot{\omega}_0 = -\frac{B_0^2R^6\sin^2(\alpha)\omega_0^3}{6I_0c^3} \tag{0.1.28}$$

$$= -\frac{2R\epsilon_{\rm A}\sin^2(\alpha)\omega_0^3}{3c}, \tag{0.1.29}$$

where α is the angle between the spin-vector and magnetic dipole. Since we expect these to be misaligned in order to observe pulsations, we can take $\sin^2\alpha \approx 1$. Taking the spin frequency as a fixed value yeilds an estimate for the spin-down frequency

$$\dot{f} = -\frac{R\omega_0^3}{3\pi c}\epsilon_{\rm A}. \tag{0.1.30}$$

In the two-state switching model, the spin-down value was observed to change by a fraction υ such that

$$\dot{f} \to \dot{f}' = (1-\upsilon)\dot{f}, \tag{0.1.31}$$

then from equation (0.1.30)

$$\epsilon_{\rm A} \to \epsilon'_{\rm A} = (1-\upsilon)\epsilon_{\rm A}. \tag{0.1.32}$$

The two-state switching changes the value of $\epsilon_{\rm A}$ and so has a knock-on effect on the effective body frame. A non-precessing NS at an angle $\beta(\epsilon_{\rm I}, \epsilon_{\rm A}, \chi)$ will, after a torque switch by a fractional amount υ, no longer be aligned with the body frame axis. This is because the effective body frame will have shifted to $\beta' = \beta(\epsilon_{\rm I}, \upsilon\epsilon_{\rm A}, \chi)$. As a result, we should expect the previously non-precessing NS to begin precessing after a torque switching event.

The NS will precess at the usual precession frequency in a cone of half-angle

$$\Delta\beta(\epsilon_{\rm I}, \epsilon_{\rm A}, \chi, \upsilon) = |\beta - \beta'|, \tag{0.1.33}$$

about the new effective body-frame axis. The expression for $\Delta\beta$ is not easily amenable to manipulation, but can easily be explored graphically. This is done in figure 0.1.8 for several choices of υ. This illustrates that the precession angle can be as much as a few degrees although it tends to zero in the limit $\epsilon_{\rm I} \gg \epsilon_{\rm A}$.

Since it is hard to gauge the significance of this we will apply it to the PSR B1828-11; a pulsar which demonstrated evidence for precession **?** and has since been reinterpreted as two-state switching (**?**). This has a frequency of $f = 2.47$ Hz, a spin-down $\dot{f} = -3.65\times10^{-13}$ Hz/s, switches are observed to occur every $T \approx 1.4$ yrs, and the spindown changes by $\upsilon = 0.71$.

We are unable to directly calculate $\Delta\beta$ from this information, since we do now know $\epsilon_{\rm I}$ or χ. Nevertheless, we can at least find the maximum allowed value found when $\chi \ll 1$ and $\epsilon_{\rm I} \sim \epsilon_{\rm A}$. This has not been found exactly although it could easily be done by maximising the function numerically. Approximately the maximum allowed angle is $\Delta\beta \sim 45^\circ$.

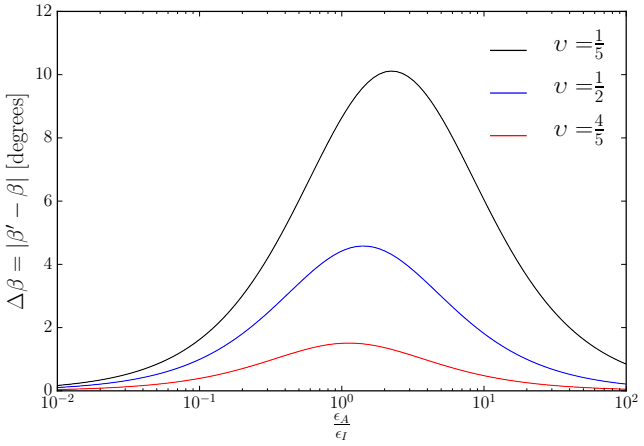

Figure 0.1.8: Illustrating the magnitude of the precession angle after switching due to the new rotation of the effect body frame. We plot the half-angle ($\Delta\beta$) of the precession cone as a function of the ratio $\epsilon_{\rm A}/\epsilon_{\rm I}$. Typically we expect real stars to have $\epsilon_{\rm A} < \epsilon_{\rm I}$.

We can now attempt to quantify the effect this may have on the timing residuals. Precession, as shown by **?**, will produce a sinusoidal variation in the residual with a magnitude given by

$$\Delta\Phi_{\rm FP} \sim \pi \cot(\chi)\theta. \tag{0.1.34}$$

This precession will be damped by other processes, but in the immediate aftermath of a switch, may be detectable.

However, when considering the residual which includes a switch we must also take into acount the effect this will have. This was considered in section (6.6) of my transfer thesis. Here we present the result that, the maximal size of phase-residuals assuming several switched occur during an observation is given by

$$\Delta\Phi_{\rm TS} \sim \frac{\pi}{16}\upsilon\dot{f}T^2, \tag{0.1.35}$$

Where T is the switching period

For PSR B1828-11 then we can directly compute the magnitude of variations in the timing residual:

$$\Delta t_{\rm TS}^{\rm B1828-11} \approx 70 \text{ ms} \tag{0.1.36}$$

This is considerably larger than the result from **?** who measured a peak to peak residual of 94 ms.